

**Steady and Transient Analysis of Flow Structures in
Tangentially Injected Turbulent Swirling Flows**

RAHUL SHARMA



DEPARTMENT OF MECHANICAL ENGINEERING

INDIAN INSTITUTE OF TECHNOLOGY DELHI

AUGUST 2025

© Copyright by Indian Institute of Technology Delhi, New Delhi 2025

All Rights Reserved

Steady and Transient Analysis of Flow Structures in Tangentially Injected Turbulent Swirling Flows

by

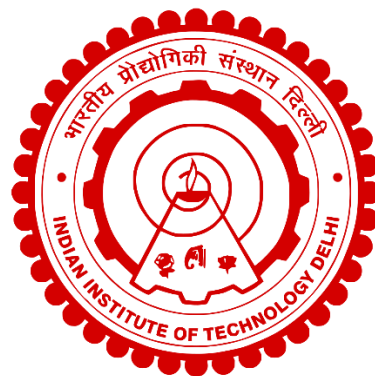
RAHUL SHARMA

Department of Mechanical Engineering

Submitted

In fulfilment of the requirements of the degree of Doctor of Philosophy

to the



INDIAN INSTITUTE OF TECHNOLOGY DELHI

AUGUST 2025

Dedicated to

My parents, sister and all those people who inspired and supported me

Certificate

The thesis entitled “**Steady and Transient Analysis of Flow Structures in Tangentially Injected Turbulent Swirling Flows**” being submitted by **Mr. Rahul Sharma** to the **Indian Institute of Technology Delhi** for the award of the degree of **Doctor of Philosophy**, is a record of original bonafide research work carried out by him. He has worked under our guidance and supervision and has fulfilled the requirements for the submission of this thesis, which has attained the standard required for a Ph.D. degree of this Institute.

The results represented in this thesis have not been submitted elsewhere for the award of any degree or diploma.

Dr. Mayank Kumar

NTPC Chair Associate Professor

Department of Mechanical Engineering

Indian Institute of Technology Delhi

Hauz Khas, New Delhi – 110016, India

Acknowledgments

I would like to express my deepest gratitude to my Ph.D. supervisor, Dr. Mayank Kumar, for their unwavering support, guidance, and encouragement throughout my research journey. Their expertise, insights, and mentorship have been invaluable in shaping my academic and professional growth.

I would like to extend my sincerest gratitude to Professor Mayank Kumar for his kindness, generosity, and willingness to help, which have been truly remarkable and have made a significant impact on my academic and personal growth. Thank you, Professor Kumar, for your unconditional support and for being such a kind and helpful person.

It gives me immense pleasure to extend my heartfelt gratitude to the members of the Student Research Committee – Prof. M. R. Ravi, Prof. P M V Subbarao, and Prof. Sawan Suman Sinha – for their insightful feedback and valuable recommendations during the SRC presentations.

I am once again deeply thankful to Prof. M. R. Ravi, the Head of the Department of Mechanical Engineering at IIT Delhi, for his unwavering institutional support throughout this endeavor.

I am very grateful to Professor Murli R. Cholehari, whose instructions and guidance played an important role in setting up and conducting the experiment. I also thank his students, Mr. Shri Hari and Aditya, for their invaluable assistance and support in setting up the PIV (Particle Image Velocimetry) equipment and conducting the experiment.

I extend my heartfelt appreciation to my dedicated lab mates, Mr. Santosh Kushwaha, Mr. Nitesh Kumar Sahu, Mr. Anurag Mishra, Ms. Ayushi Mishra, Mr. Sanjay, Mr. Hitesh Kumar Gupta, Mr. Vikas Jangir and Mr. Ramendra Kumar, for their never-ending support

throughout my academic journey at IIT Delhi. Their contributions have enriched my research experience and made it more fulfilling.

Special thanks are due to Mr. Sandeep Lamba, Mr. Abhishek Kandpal and Mr. Govind Sharma for their encouragement and friendship throughout this journey.

I am deeply indebted to all the individuals mentioned above for their unwavering support and encouragement, which has played a significant role in the successful completion of my research.

Thank you.

Rahul Sharma

ABSTRACT

Swirling flows play a crucial part in the gas phase and solid particle combustion in the most practical burners and furnaces. This research presents a detailed steady and unsteady computational investigation of the swirling flows in a confined domain with tangential injections. The swirling flow inside the confined domain is highly turbulent and coupled as compared with axial bulk flow, resulting in complex flow dynamics. The study explores the distribution of swirl intensity and flow structures, i.e., Vortex core, Internal Recirculation Zones (IRZ) for both isothermal and reacting environments, aiming to enhance a better understanding of flow characteristics in furnaces and burners. Simple circular and square cylindrical geometries with four tangential injections are considered for investigation. The evolution of swirl intensity is analyzed with and without accounting for the effects of accompanying pressure fluctuations. Turbulence is modeled using the Shear Stress Transport (SST) $k-\omega$ model followed by validation studies for steady and unsteady conditions.

The findings indicate that the injection angle significantly influences the strength of swirl induced by such tangential injections but remains relatively constant across different bulk flow Reynolds numbers (Re), except for lower Re values. The formation of swirling flow leads to the creation of IRZ at injection angles of 6° and above, or when the asymptotic value of the maximum Swirl Number in the domain exceeds approximately 0.6, mirroring the transition value of inlet Swirl Number in swirling flows with axial injections. The length of the IRZ increases with the injection angle and varies with Re for lower Re values at a given injection angle but stabilizes for higher values above 40000 in isothermal condition. Whereas incorporating heat addition effect by creating reacting environment in the swirling flow, leads to no effect of Re on length of IRZ. The

conventional Swirl Number exhibits a rapid increase downstream of the injection plane followed by a gradual decline. In contrast, an alternative Swirl Number, which incorporates gauge pressure variation, shows a consistent, gradual decrease downstream of the injection plane. This alternative Swirl Number, incorporating the gauge pressure term, encompasses the interconversion between axial momentum and pressure in regions of vortex breakdown and IRZ formation, providing an alternative perspective on the evolution of swirl intensity in swirling flows. The higher heat addition flattens the swirling strength distribution and shrinks the size of IRZ. Interestingly, variations in operating pressure have no noticeable effect on the swirl strength distribution or the size of IRZ.

The simulations demonstrate that swirling flows exhibit a statistically steady behavior (no large-scale unsteadiness) within the circular confined domain, while the flow inside the square cylindrical confined domain displays transient characteristics of mean flow (large-scale unsteadiness). The time-dependent nature of the flow leads to the formation of complex flow structures such as asymmetrical vortex cores and IRZ, as well as the precession of vortex cores and oscillation of IRZ along the central axis. Conclusively the precession frequencies of vortex core are directly dependent on the swirling strength and Reynold number.

सारांश

घूर्णीय प्रवाह (Swirling Flows) अधिकांश व्यावहारिक बर्नर और भट्टियों में गैस चरण और ठोस कण दहन में एक महत्वपूर्ण भूमिका निभाते हैं। यह शोध सीमित क्षेत्र (confined domain) में स्पर्शीय (tangential) इंजेक्शन के साथ होने वाले घूर्णीय प्रवाह की स्थिर (steady) और अल्पकालिक (unsteady) संगणकीय (computational) जाँच को विस्तारपूर्वक प्रस्तुत करता है। सीमित क्षेत्र के भीतर का घूर्णीय प्रवाह अत्यधिक अशांत (turbulent) होता है और यह अक्षीय बल्क प्रवाह की तुलना में अधिक युग्मित (coupled) होता है, जिससे जटिल प्रवाह गतिकी उत्पन्न होती है।

अध्ययन में घूर्णी तीव्रता (swirl intensity) और प्रवाह संरचनाओं जैसे कि वॉर्टेक्स कोर (vortex core), आंतरिक पुनरावर्तन क्षेत्र (IRZ) का वितरण, दोनों ही समतापीय (isothermal) और दहनशील (reacting) परिस्थितियों में, समझने का प्रयास किया गया है ताकि भट्टियों और बर्नरों में प्रवाह विशेषताओं की बेहतर समझ प्राप्त की जा सके। अध्ययन के लिए चार स्पर्शीय इंजेक्शन के साथ सरल गोल और वर्गाकार बेलनाकार ज्यामितियाँ (circular and square cylindrical geometries) चुनी गई हैं।

घूर्णी तीव्रता के विकास का विश्लेषण दबाव उतार-चढ़ाव (pressure fluctuations) के प्रभावों को शामिल कर और बिना शामिल किए किया गया है। अशांति (turbulence) का मॉडलिंग Shear Stress Transport (SST) $k-\omega$ मॉडल का उपयोग कर किया गया है, जिसे स्थिर और अल्पकालिक स्थितियों के लिए सत्यापन अध्ययन द्वारा परखा गया है।

परिणाम दर्शाते हैं कि इंजेक्शन कोण (injection angle) घूर्णी प्रवाह की तीव्रता को काफी प्रभावित करता है, लेकिन यह बल्क प्रवाह रेनॉल्ड्स संख्या (Re) के विभिन्न मानों पर तुलनात्मक

रूप से स्थिर रहता है, सिवाय कम Re मानों के। घूर्णीय प्रवाह का निर्माण इंजेक्शन कोण 6° या उससे अधिक पर IRZ के निर्माण की ओर ले जाता है, या जब क्षेत्र में अधिकतम घूर्णी संख्या (Swirl Number) का अपरास्मित मान (asymptotic value) लगभग 0.6 से अधिक हो जाता है, जो अक्षीय इंजेक्शन के साथ होने वाले प्रवाह में इनलेट Swirl Number के संक्रमण मान से मेल खाता है।

IRZ की लंबाई इंजेक्शन कोण के साथ बढ़ती है और दिए गए कोण पर कम Re मानों के लिए बदलती रहती है, लेकिन isothermal स्थिति में $Re > 40000$ के बाद स्थिर हो जाती है। वहीं, जब दहनशील वातावरण बनाकर ऊष्मा वृद्धि (heat addition) को शामिल किया जाता है, तो Re का IRZ की लंबाई पर कोई प्रभाव नहीं देखा गया।

पारंपरिक Swirl Number इंजेक्शन तल के बाद तेजी से बढ़ता है और फिर धीरे-धीरे घटता है। इसके विपरीत, एक वैकल्पिक Swirl Number, जो गेज दबाव (gauge pressure) में भिन्नता को शामिल करता है, इंजेक्शन तल के बाद लगातार और क्रमिक रूप से घटता है। यह वैकल्पिक Swirl Number, जो गेज दबाव पद को शामिल करता है, वह उन क्षेत्रों में अक्षीय संवेग (axial momentum) और दबाव के बीच अंतःपरिवर्तन को दर्शाता है जहाँ वॉर्टेक्स विघटन (vortex breakdown) और IRZ का निर्माण होता है, जिससे घूर्णी तीव्रता के विकास की एक वैकल्पिक समझ मिलती है।

अधिक ऊष्मा जोड़ने से घूर्णीय तीव्रता का वितरण समतल हो जाता है और IRZ का आकार घट जाता है। रोचक रूप से, परिचालन दबाव (operating pressure) में भिन्नता का घूर्णीय तीव्रता वितरण या IRZ के आकार पर कोई स्पष्ट प्रभाव नहीं पड़ता।

सिमुलेशन से पता चलता है कि गोल सीमित क्षेत्र के भीतर घूर्णीय प्रवाह सांख्यिकीय रूप से स्थिर व्यवहार (statistically steady behavior) प्रदर्शित करता है (कोई बड़े पैमाने की अनियतता नहीं होती), जबकि वर्गाकार सीमित क्षेत्र में प्रवाह औसत प्रवाह की क्षणिक विशेषताएं (transient characteristics) प्रदर्शित करता है। प्रवाह की समय-निर्भर प्रकृति जटिल प्रवाह संरचनाओं का निर्माण करती है, जैसे कि विषम वॉर्टेक्स कोर, IRZ का निर्माण, साथ ही वॉर्टेक्स कोर का प्रीसेशन (precession) और IRZ का केंद्रीय धुरी के साथ दोलन (oscillation)। निष्कर्षतः, वॉर्टेक्स कोर की प्रीसेशन आवृत्तियाँ सीधे घूर्णीय तीव्रता और रेनॉल्ड्स संख्या पर निर्भर होती हैं।

Table of Contents

Certificate	i
Acknowledgments	ii
ABSTRACT	iv
सारांश	vi
Table of Contents	ix
List of Figures.....	xi
List of Tables	xvi
Nomenclatures.....	xvii
1. INTRODUCTION	1
2. LITERATURE REVIEW	5
2.1. Swirl Characterization	6
2.2. Numerical Simulation and CFD Studies Overview	7
2.3. Impact of Swirl on the Flow Field and Fundamental Flow Structures	8
2.4. Influence of Geometry and Time-Dependent Behavior of Swirling Flow	9
2.5. Characterization of Periodic Asymmetric Behavior in Swirling Flows.....	11
2.6. Gaps Identified from the Literature Reviewed.....	13
2.7. Objectives of the present work	14
3. METHODOLOGY	15
3.1. Physical and computational domain	15
3.1.1. Straight circular cylinder (Circular domain)	16
3.1.2. Straight square cylinder (Square domain).....	17
3.2. Selecting Simulation Approach	19
3.2.1. Domain-Wise Detection of large-scale unsteadiness via URANS Simulations	19
3.2.1.1. Straight Circular Cylindrical Domain.....	19
3.2.1.2. Straight Square Cylindrical domain.....	22
3.2.2. Comparison of mean flow field obtained from validated RANS model with LES results 24	
3.2.2.1. Circular confined domain	24
3.2.2.2. Square confined domain	26
3.3. Simulation Case Matrix for Circular and Square Geometries	28
3.4. Post Processing Approach.....	31
3.4.1. Vortex Core Identification and visualization.....	31
4. STEADY SWIRLING FLOW IN THE CONFINED DOMAIN.....	34
4.1. Isothermal Flow	34

4.1.1.	Governing equations and numerical methods	35
4.1.2.	Model validation	36
4.1.3.	Results and discussion	39
4.1.3.1.	Evolution of swirl intensity	39
4.1.3.2.	Swirling flow regimes	44
4.2.	Reacting Flow	49
4.2.1.	Basic modeling and other operating parameters	49
4.2.2.	Results and discussion	52
4.2.2.1.	Impact of mass flow and injection angle on evolution of swirl strength	52
4.2.2.2.	Swirling flow regimes	55
4.2.2.3.	Effect of operating pressure and heat addition	59
5.	UNSTEADY SWIRLING FLOW	64
5.1.	Numerical considerations	65
5.2.	Model Validation	67
5.3.	Results and discussion	71
5.3.1	Temporal variation of flow variables	72
5.3.2	Flow visualization	77
5.3.3	Normalized precession frequencies and swirl number	81
6.	CONCLUSIONS	86
7.1	Steady swirling flow in straight circular cylinder in isothermal environment	86
7.2	Steady swirling flow with heat addition and variable operating pressure	87
7.3	Transient behaviour of swirling flow	88
	FUTURE WORK	89
	References	90
	Appendix A	98
	Appendix-B	110
	Appendix-C	112

List of Figures

Figure 2.1 Methods of swirl generation in the furnace in (a) Swirl burner (SB) and (b) Tangentially Injected Burner (TIB)	5
Figure 3.1 Schematic diagram of the cylindrical domain with four symmetric tangential injectors, α is the injection angle	16
Figure 3.2 Discretized cylindrical domain with four square injectors	17
Figure 3.3 Schematic diagram of the square confined domain with four injectors offset from the wall center.....	18
Figure 3.4 The discretized image of the domain with four injectors.....	18
Figure 3.5 Graphs representing the variation of residuals, vertex average axial velocity, vertex average turbulent kinetic energy and periodic fluctuation of axial velocity (top-left to bottom-right) against flow iterations with time step integration.....	23
Figure 3.6 Comparison of mean axial velocity profiles for LES and RANS results along the radial direction at axial locations 0.3D, 0.6D and 1D downstream from the injection plane	25
Figure 3.7 Comparison of mean axial velocity profiles at two different axial locations obtained from the LES and RANS simulations performed on square confined domain	26
Figure 3.8 FFT spectrum plots for both test cases simulated using LES and URANS modeling.....	27
Figure 3.9 Visualization of vortex core for validation case (top left) and for current case of square domain	32
Figure 3.10 Use of planer velocity or tangential velocity to generate isosurface showing the shape and size of PVC	33
Figure 4.1 Distribution of axial velocity on the central axis of the domain for three different mesh resolutions	35

Figure 4.2(a) Illustrative diagram of the dump combustor with swirler and inlet pipe arrangement [25], [52] (b) View of discretized SB geometry mesh in current validation case	37
Figure 4.3 Distribution of predicted axial velocity, normalized by U_{ref} (19.2 m/s) for all turbulence models considered along with experimental data (a) at the plane 2H distance, (b) 15H distance from the combustor inlet and (c) along the central axis	38
Figure 4.4 Distribution of (a) Swirl number (S), Axial flux of axial momentum, axial flux of angular momentum and static gauge pressure, (b) Gradient of axial momentum and area-weighted average static pressure along with normalized axial distance for Re 71900 and injection angle 10° , (c) Zoomed view plot of Fig. 4.4 (b) for specific range from 3D to 8.5D	42
Figure 4.5 Contours of static gauge pressure(N/m^2), axial momentum(N/m^2) and angular momentum(N/m) at the multiple sections of the domain for Re 71900 and injection angle 10°	42
Figure 4.6 Distribution of Swirl number (S) along with normalized axial distance for various bulk flow Reynolds number (mentioned in the legend) considered, for injection angles (a) 5° (b) 7° (c) 10° (d) 15° (e) 20° (f) 25°	43
Figure 4.7 Distribution of S_P and S along with normalized axial distance for Re 71900, while keeping injection angle at (a) 5° (b) 7° (c) 10° (d) 15° (e) 20° (f) 25°	43
Figure 4.8 Distribution of (a) S_{max} and (b) $S_{p,max}$ observed for all range of Reynolds number (calculated based on domain diameter) considered. Re scale is normalized by 1000 just to represent the axis value in lower range	45
Figure 4.9 (a) Normalized IRZ length v/s injection flow Re for various injection angles (b) Asymptotic value of the normalized IRZ length v/s corresponding asymptotic values of S_{max} and $S_{p,max}$	46

Figure 4.10 Contours of negative axial velocity on a central plane representing IRZ for all range of injection angle considered and corresponding asymptotic maximum swirl number (S_{\max} and $S_{P,\max}$) for Reynolds number (a) 7190 (b) 71900 on the scale normalized by cylinder diameter 0.3m.....	47
Figure 4.11A Distribution of Swirl number (S) along with normalized axial distance for various bulk flow Reynolds number (mentioned in the legend) considered, for injection angles (a) 15° (b) 25° (c) 35° (d) 45° (e) 55° keeping operating pressure 1 bar and 2 MJ/kg-mixture heat addition.....	54
Figure 4.12 Distribution of maximum (a) S_{\max} and (b) $S_{P,\max}$ observed for all the injection mass flow range considered at 1 bar operating pressure and 2 MJ/kg-mixture heat addition.....	56
Figure 4.13 Variation of length of IRZ with bulk flow Reynolds number and injection angle	57
Figure 4.14 Contours of negative axial velocity on a central plane representing IRZ for all range of injection angles for Reynolds number (a) 4930 and (b)19700 at 1 bar operating pressure, 2 MJ/kg-mixture heat addition. The geometrical scale is normalized by cylinder diameter.	58
Figure 4.15 Impact of heat addition on Swirl number distribution (a) S (b) S_P for operating pressures 1 bar and 5 bar, injection angle 25° and 19700 Re.....	60
Figure 4.16 Impact of operating pressure and heat addition on IRZ shape and size for 19700 Re and injection angle 25° on central plane for heat addition from 0 to 7 MJ/kg-mixture for operating pressure (a) 1 bar and (b) 5 bar	62
Figure 5.1 Plots of (a) All scaled residuals, (b) Axial velocity monitor, and (c) Turbulent kinetic energy monitor at a point on center line of the domain with iterations, representing convergence at each time step	66

Figure 5.2 Distribution of axial velocity on the central axis of the domain for three different mesh resolutions	67
Figure 5.3 (a) Illustrative diagram of the dump combustor with axial swirler and inlet pipe arrangement (Taamallah et al., 2019) [31] (b) Discretized domain with 0.288 M structured mesh elements	68
Figure 5.4 Comparison of predicted non-reacting mean axial velocity profiles with experimental data [1] and LES data [1] in the radial direction at a location (a) $z/R = 0$ and (b) $z/R = 0.5$ downstream from the expansion plane.....	69
Figure 5.5 FFT of transient data of axial velocity fluctuation at a point 0.038 m downstream of swirler plane	69
Figure 5.6 Instantaneous flow velocity temporal patterns at point $0.4D_e$ for $12500 Re_\theta$ and all swirl numbers.....	74
Figure 5.7 Limit cycles for $12500 Re_\theta$ at point $0.4D_e$	75
Figure 5.8 Instantaneous flow velocity temporal patterns at point $0.4D_e$ for $62500 Re_\theta$ and all swirl numbers.....	76
Figure 5.9 Limit cycles for $62500 Re_\theta$ at point $0.4D_e$	77
Figure 5.10 Instantaneous velocity vectors at multiple cross sections downstream from the injection plane with vorticity contour for $12500 Re_\theta$	78
Figure 5.11 Instantaneous velocity vectors at multiple cross sections downstream from the injection plane with vorticity contour for $62500 Re_\theta$	79
Figure 5.12 Instantaneous iso-surface of tangential velocity (0.02 m/s) and axial velocity (0 m/s) representing the vortex core and IRZ, respectively, for $62500 Re_\theta$ and $9.59 S_G80$	
Figure 5.13 Variation of IRZ length (mean) with Swirl number	81
Figure 5.14 Visualization of IRZ through mean flow field representing the contour of only negative axial velocity region at the central plane along the length of the domain	81

Figure 5.15 (a) FFT analysis plot of temporal velocity data for the case of 12500 Re_θ and 10.57 S_G (b) Variation of Strouhal Number with S_G	83
Figure 5.16 Pictorial representation of the effect of the Swirl number on the flow direction (Swirl direction) and the precession direction.....	84

List of Tables

Table 3-1 Operating and boundary conditions for URANS simulation of straight circular cylinder	20
Table 3-2 Temporal plots of vertex average axial velocity and turbulent kinetic energy for test case at a point on the central axis of circular domain	21
Table 3-3 Operating and boundary conditions for URANS simulation of straight square cylinder test case.....	22
Table 3-4 Comparison of most dominating frequency obtained from FFT plots in figure 3.8	28
Table 3-5 Simulation case matrix for circular domain	29
Table 3-6 Simulation case matrix for square domain.....	30
Table 4-1 Asymptotic swirl number independent of flow Reynolds number for the given injection angle and geometry.....	44
Table 5-1 Comparison of predicted axial velocity fluctuation frequency from RANS simulation with experimental and LES results of taamallah et al. 2019 [1].....	70
Table 5-2 All offsets are converted into corresponding geometric swirl numbers	71

Nomenclatures

D	Diameter of the domain (m)
D_e	Sides of the square confined domain (m)
D_o	Tangential Circle Diameter (m)
G_x	Axial flux of linear momentum (kg-m/s ²)
G'_x	Total axial flux of linear momentum(kg-m/s ²)
G_θ	Axial flux of angular momentum (kg-m ² /s ²)
L	Length of the cylindrical domain (m)
p	Pressure (N/m ²)
P	Static pressure (N/m ²)
R	Exit radius (m)
Re	Reynolds number
S	Swirl Number
S_h	Source term due to radiation, homogeneous reactions, and exchange of energy between phases (kg/m-s ³)
S_p	Swirl Number considering pressure
S_G	Geometric Swirl Number
A_T	Tangential injection area (m ²)
T	Mean temperature (K)
T'	Fluctuating temperature component (K)
U	Axial velocity component (m/s)
u_i	Average velocity components (m/s)
u_i'	Fluctuating velocity component (m/s)
W	Tangential velocity component (m/s)
λ	Gas-phase thermal conductivity (W/m-K)
ρ	Density of the fluid (kg/m ³)
δ_{ij}	ij^{th} component of Kronecker-delta tensor
μ	Dynamic viscosity (kg/m-s)
Φ	Viscous dissipation (1/s ²)
c_p	Specific heat per unit mass flow (J/kg-K)
S_{max}	Maximum Swirl Number observed in the domain

$S_{P,max}$	Maximum Swirl Number observed in the domain with pressure inclusion
\vec{v}	Velocity vector (m/s)
Y_i	Mass fraction of i^{th} species
J_i	Diffusion flux of i^{th} species
$D_{i,m}$	Mass diffusion coefficient for species in the mixture
$D_{T,i}$	Thermal diffusion coefficient
R_i	Net rate of production of species by chemical reaction
S_i	Rate of creation by addition from any user defined sources
Sc_t	Turbulent Schmidt Number
μ_t	Turbulent viscosity
Re_θ	Reynolds Number calculated from tangential velocity
St	Strouhal Number
f	Frequency (1/s)
D_h	Hydraulic diameter (m)
Q	Volumetric flow rate (m ³ /s)

Acronyms

SN	Swirl Number
SBs	Swirl Burners
TIBs	Tangential Injection Burners
CRZ	Central Recirculation Zone
IRZ	Internal Recirculation Zone
RANS	Reynolds Average Navier Stokes
SST	Shear Stress Transport
FFT	Fast Fourier Transform
PIV	Particle Image Velocimetry
SLPM	Standard Liter Per Minute
PVC	Precessing Vortex Core
CFD	Computational Fluid Dynamics